

Assessment of the Effects of Online Linear Leak Current Compensation at Different Pacing Frequencies in a Dynamic Action Potential Clamp System

Alan Fabbri¹, Adrianus Prins¹, Teun P de Boer¹

¹ Department of Medical Physiology, Division of Heart & Lungs, University Medical Center Utrecht, Utrecht, The Netherlands

Abstract

Dynamic action potential (AP) clamp (dAPC) is an electrophysiology technique that allows one to study in real time the effects of a biological current included in a computational AP model. During an experiment, the seal resistance between the cell membrane and the pipette is finite and a leak current (I_{leak}) occurs. Its reduction is crucial to properly assess the effect of a drug. Our work aims to quantify the impact of I_{leak} on a ventricular AP model and to evaluate the benefits of an online compensation.

We adopted the Ten Tusscher 2006 as human ventricular model. We used a passive model cell ($C_m = 19.8\text{pF}$, $R_{seal} = 500\text{M}\Omega$) and online compensated the leak current through a linear model. V_{max} , RMP and $APD_{20,50,90}$ are measured at several degrees of compensation (within 0 and 100%), at the pacing frequencies of 0.5, 1 and 2 Hz, and compared with the scenario in which there is no connection between the model cell and the AP model.

I_{leak} decreases V_{max} , depolarizes RMP (up to +6.1mV at 1 Hz) and prolongs APD; a full compensation of I_{leak} brings the AP biomarkers close to the open loop condition.

With this test, we show that online compensation of I_{leak} is beneficial for proper assessment of AP biomarker. The correction of RMP is key, as it affects the following phases of the AP.

1. Introduction

Dynamic Clamp (DC) is a hybrid electrophysiology technique that allows one to link a real cell with a computational model, in real time [1]. In the dynamic Action Potential clamp (dAPC) configuration, a cell overexpressing a specific ion channel (e.g Human Embryonic Kidney (HEK, [2]) or Chinese Hamster Ovary (CHO, [3]) cells), is coupled with a whole cell action potential (AP) computational model. In this setting, the membrane potential of the computational model stimulates the ion channel overexpressed in the real cell, as would happen in a real car-

diomyocyte. In turn, the ion current generated in the real cell is scaled appropriately and fed back into the computational model, thereby contributing to action potential formation, and therefore to the final AP waveform, forming a closed-loop system. As result, dAPC improves on classical electrophysiology techniques as it enables observation of the effects of a drug on the current of interest, and on the AP at the same time.

During a dAPC experiment, the resistance between the pipette and the cell membrane (R_{Seal}) is finite and a leak current (I_{leak}) occurs. In voltage clamp experiments, the I_{leak} artifact can be corrected for during post-processing. Since dAPC is a real time technique, the I_{leak} must be handled during the experiments. An online compensation avoids misleading effects on the AP waveform.

This study aims to quantify the effects of I_{leak} and the benefits of online compensation when using a ventricular computational AP model in a dAPC experiment.

To do that, we compared five AP biomarkers (Resting Membrane Potential, RMP, Maximal upstroke Velocity, V_{max} , and AP Duration at 20,50 and 90% of repolarization, $APD_{20,50,90}$) for several degrees of I_{leak} online compensation (0% (No compensation), 25%, 50%, 75% and 100%) at three pacing frequencies (0.5 Hz, 1 Hz and 2 Hz), adopting the open loop configuration (no I_{leak} injection) as a reference.

2. Methods

2.1. The dynamic AP clamp system

In this study we used a prototype developed in our lab of the Nanion Patchliner Dynamite⁸ [4], adapted to the dAPC configuration and running the endocardial version of the ten Tusscher and Panfilov 2006 ventricular model (TP06, endo) [5]. The adoption of the Rush-Larsen method [6] allows one to provide a real time stable solution of TP06, splitting the set of ordinary differential equations in two groups: the time course of the gating variables is described via their analytic, exponential solutions; all the other state variables are integrated through the Forward Euler method

with a step time of 50 μs .

2.2. The model cell and the leak current compensation

In our dAPC experiment, the HEKA MC10 model cell (HEKA Elektronik, Germany) provides the external current that affects the final shape of the AP. The MC10 model cell consists in a passive linear parallel RC circuit ($R_{MC} = 500M\Omega$ and $C = 19.8pF$). We assumed $R_{MC} = R_{leak}$, therefore, the model cell contributes to the AP shape providing I_{leak} . The linear components of the model cells allowed us to perform the online I_{leak} compensation through a linear model [7]:

$$I_{comp} = \alpha_{comp} g_{leak} (V_m - E_{leak}) \quad (1)$$

$$I_{final} = I_{leak} - I_{comp} \quad (2)$$

During the diastolic interval, the current density provided by the model cell was $\approx 8pA/pF$, a value that wouldn't allow the TP06 to repolarize. For this reason the injected current was scaled down of a factor 1/10.

2.3. Hardware and software

We carried out the dAPC experiments on a EPC10-USB amplifier controlled by Patchmaster v2x90.2 (HEKA Elektronik, Germany). Data analysis and plots (extraction of the AP biomarkers $APD_{20,50,90}$, RMP and V_{max}) are performed with custom code using Matlab 2017b (The Mathworks, Natick MA, USA).

To provide a more in depth analysis of the mechanisms responsible for the changes of the AP biomarkers, we ran simulations of the TP06 model using OpenCOR [8], reproducing the effects of the leak current with the same properties of the HEKA MC10 model cell.

3. Results

The effects of I_{leak} on the AP morphology at 0.5, 1 and 2 Hz are shown in Figure 1,2 and 3. If not compensated, I_{leak} depolarizes RMP (see panels C, Figure 1,2 and 3), dampens the peak (panels D) and prolongs the late repolarization phase (panels E). The online compensation of I_{leak} progressively brings the AP shape back to the open loop condition, with a good superimposition when a full compensation is performed.

The biomarker extraction reveals a RMP depolarization similar for the three frequencies, with the highest variation at 1 Hz ($RMP_{0\%} = -78.1mV$, $RMP_{OpenLoop} = -84.2mV$, $\Delta RMP = +6.1mV$, $\Delta RMP\% = +7.2\%$). V_{max} monotonically decreases with faster pacing ($\Delta V_{max} = -18.3, -26.9$ and -30.7% at 0.5, 1 and 2 Hz

respectively.). For a complete overview see Table 1). The APD undergoes to prolongation both in early and in late repolarization (see Table 2). Surprisingly APD_{20} lengthens between +24 and +26.2% (at 2 and 0.5 Hz respectively). At first sight, indeed, one could expect a faster repolarization due to the outward I_{leak} , instead of a slower one. The underlying mechanisms will be explained in the Discussion section. Finally, APD_{50} and APD_{90} show smaller increases ($\Delta APD_{50} = 4.4\%$ at 0.5 Hz, $\Delta APD_{90} = 5.5\%$ at 2 Hz.)

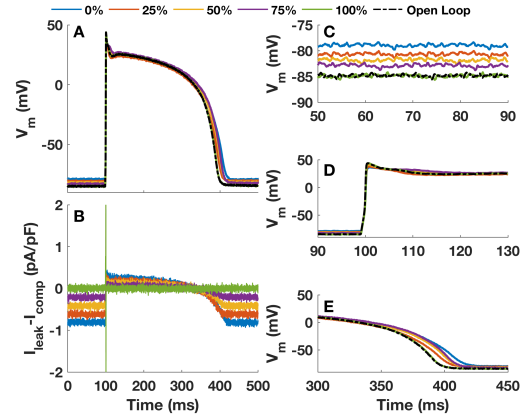


Figure 1. A-B) AP and injected current. C) RMP, D) Upstroke and peak, E) late depolarization of TP06 at 0.5 Hz

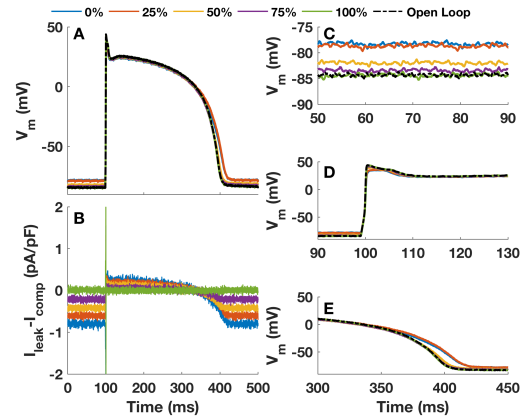


Figure 2. A-B) AP and injected current. C) RMP, D) Upstroke and peak, E) late depolarization of TP06 at 1 Hz

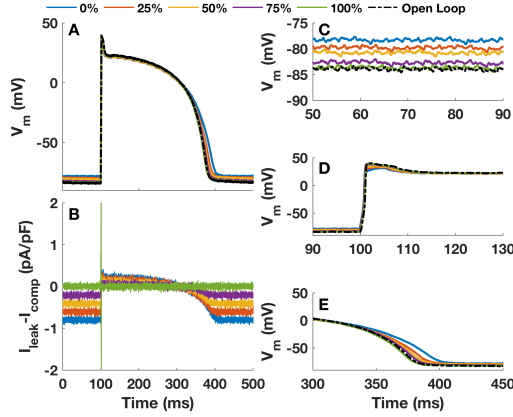


Figure 3. A-B) AP and injected current. C) RMP, D) Upstroke and peak, E) late depolarization of TP06 at 2 Hz

Table 1. V_{max} , RMP and relative changes with respect to the open loop condition at 0.5, 1 and 2 Hz

		V_{max}	ΔV_{max}	RMP	ΔRMP
		V/ms	%	mV	%
0.5 Hz	0%	248	-18.3	-79.0	6.9
	25%	268	-11.8	-80.6	4.9
	50%	291	-4.3	-81.7	3.6
	75%	308	1.1	-81.8	3.6
	100%	304	0.1	-84.9	-0.1
	Open Loop	304		-84.8	
1 Hz	0%	224	-26.9	-78.1	7.2
	25%	233.	-23.9	-78.5	6.8
	50%	284	-7.1	-81.9	2.8
	75%	291	-5.0	-83.3	1.1
	100%	303	-1.1	-84.5	-0.3
	Open Loop	306		-84.2	
2 Hz	0%	187	-30.7	-78.2	6.9
	25%	214	-20.4	-79.7	5.1
	50%	231	-14.1	-80.8	3.8
	75%	260	-3.6	-82.7	1.5
	100%	265	-1.8	-83.8	0.3
	Open Loop	269		-84.0	

4. Discussion and Conclusion

With this study, we aimed to quantify the impact of linear I_{leak} on the AP morphology of an in real time running ventricular computational model (TP06,endo [5]), integrated in a dAPC setup. To do that, we performed the online I_{leak} compensation at increasing degrees (from 0 to 100%) at 0.5, 1 and 2 Hz, and we compared several AP biomarkers.

The results showed that I_{leak} depolarizes RMP, decreases V_{max} and prolongs APD both during early and late repolarization in all the explored pacing frequencies. The full online compensation brings the biomarkers close to the open loop condition, where no current is injected.

To investigate the underlying mechanisms, we performed simulations mimicking the experimental condi-

Table 2. $APD_{20,50,90}$ and relative changes with respect to the open loop condition at 0.5, 1 and 2 Hz

		APD_{20}	ΔAPD_{20}	APD_{50}	ΔAPD_{50}	APD_{90}	ΔAPD_{90}
		ms	%	ms	%	ms	%
0.5 Hz	0%	179.2	26.2	276.2	4.4	309.4	5.4
	25%	165.2	16.4	268.3	1.4	300.6	2.4
	50%	157.7	11.1	272.7	3.1	303.6	3.5
	75%	148.3	4.5	275.3	4.1	305.8	4.2
	100%	143.9	1.4	265.2	0.2	293.7	0.1
	Open Loop	142.0		264.6		293.4	
1 Hz	0%	179.8	23.6	275.0	2.3	309.9	7.2
	25%	180.6	24.1	278.0	3.4	310.9	6.8
	50%	160.7	10.4	269.1	0.1	301.8	2.8
	75%	153.7	5.7	268.0	-0.3	299.3	1.1
	100%	148.4	2.0	268.6	-0.1	298.7	-0.3
	Open Loop	145.5		268.8		299.1	
2 Hz	0%	169.0	24.0	256.3	4.2	292.8	5.5
	25%	161.7	18.6	251.3	2.2	286.0	3.1
	50%	156.9	15.2	249.5	1.5	282.4	1.8
	75%	145.5	6.8	247.9	0.8	280.3	1.0
	100%	140.8	3.4	244.6	-0.5	275.9	-0.6
	Open Loop	136.3		245.9		277.5	

tions. Using OpenCOR [8], we observed the uncompensated I_{leak} scenario (see Figure 4, red lines) with the original model (black lines), and we compared the time course of I_{Na} and all the other membrane currents. The depolarized RMP inactivates I_{Na} ion channels, leading to halved I_{Na} peak (see Figure 4, panel B). The simulations without compensation of I_{leak} showed a marked decrease of the fast (h) and slow (j) inactivation variables before and during the I_{Na} peak (see Figure 4, panel E,F and G), for all the three frequencies. The activation gate m showed a slight decrease at 0.5 and 1 Hz (-0.35 and -2.4% respectively), whereas it undergoes to an increase of 13% at 2 Hz, compensated by a larger decrease of h and j. The reduced peak of I_{Na} is therefore responsible for the decreased V_{max} .

During the plateau phase, the time course of the net current in the two scenarios is similar (see Figure 4 panel C) and the repolarization rate is almost the same. This result is achieved by an interplay between the inward net current and I_{leak} : the model reacts to I_{leak} providing a slightly stronger inward current during the early stage of the repolarization (see Figure 4, panel D). APD_{20} shows an unexpected prolongation due to a smaller AP amplitude (AP peak - RMP), rather than a more intense net inward current. I_{leak} slows down the late repolarization due to its inward contribution, which is responsible for a delayed and less intense repolarizing current.

The discussed results were obtained using a specific computational model (TP06). As a further step it would be fruitful to quantify the impact of I_{leak} on different computational models (e.g. on the O'Hara-Rudy 2011 model [9], one of the latest and most used models). The AP waveform results from a delicate balance between a specific mix of currents, and the adoption of a different model could lead to different behaviors.

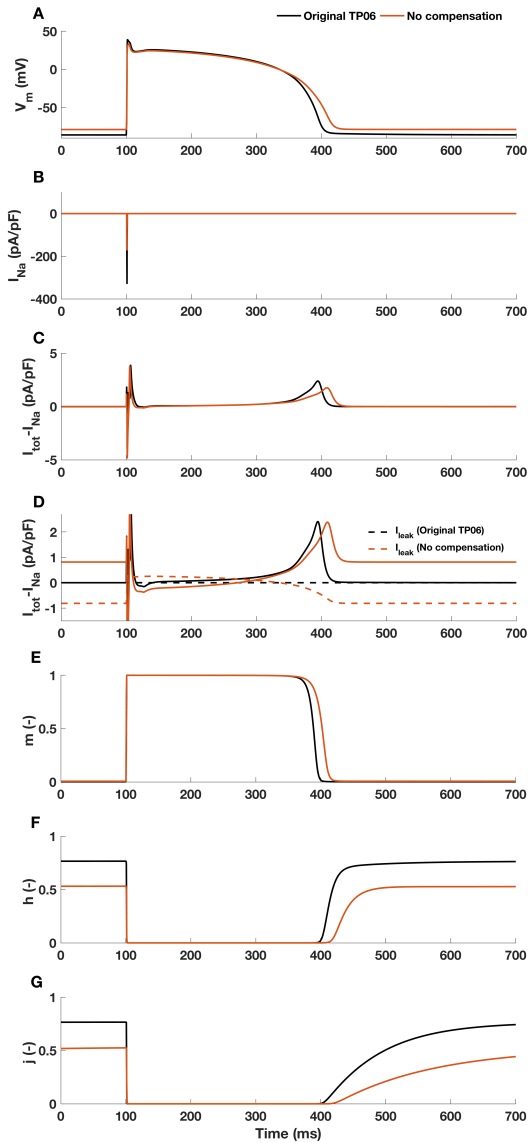


Figure 4. Underlying mechanisms responsible for changes in AP morphology. Time course of A) AP, B) I_{Na} , C) total net current without I_{Na} , D) total net current (solid lines) and leak current (dashed lines) displayed separately. Time course of E) activation gate m , F) fast inactivation gate h and G) slow inactivation gate j of I_{Na} . Pacing frequency = 1 Hz but the same mechanisms hold true at 0.5 and 2 Hz.

From the experimental perspective, our approach with the model cell allowed us to assess the effect of I_{leak} with a R_{Seal} value that is known and remains stable over time. This is an ideal condition that does not usually occur during an experiment with HEK or CHO cells. Our dAPC system allows the user to automatically update the current estimated value of R_{Seal} , which typically decreases over

time. In conclusion, online compensation of I_{leak} is important in dAPC experiments to avoid inaccurate results that are due to artifacts present in the experimental setup.

Acknowledgments

The authors thank Dr. Gary Mirams (The University of Nottingham) for the valuable help regarding the Rush-Larsen method. This research is financially supported by MKMD grants with project numbers 114021501 and 114022502 (ZonMW).

References

- [1] Wilders R. Dynamic clamp: a powerful tool in cardiac electrophysiology. *The Journal of Physiology* 2006;576(2):349–359.
- [2] Thomas P, Smart TG. HEK293 cell line: A vehicle for the expression of recombinant proteins. *Journal of Pharmacological and Toxicological Methods* 2005;51(3):187–200.
- [3] Gamper N, Stockand JD, Shapiro MS. The use of chinese hamster ovary (CHO) cells in the study of ion channels. *Journal of Pharmacological and Toxicological Methods* 2005; 51(3):177–185.
- [4] Becker N, Horváth A, Boer TD, Fabbri A, Grad C, Fertig N, George M, Obergrussberger A. Automated dynamic clamp for simulation of IK1 in human induced pluripotent stem cell-derived cardiomyocytes in real time using patch-clamp dynamite8. *Current Protocols in Pharmacology* 2020; 88(1):e70.
- [5] ten Tusscher KHWJ, Panfilov AV. Alternans and spiral breakup in a human ventricular tissue model. *American Journal of Physiology Heart and Circulatory Physiology* 2006; 291(3):H1088–H1100.
- [6] Marsh ME, Ziaratgahi ST, Spiteri RJ. The secrets to the success of the rush-larsen method and its generalizations. *IEEE Transactions on Biomedical Engineering* 2012;59(9):2506–2515.
- [7] Ahrens-Nicklas RC, Christini DJ. Anthropomorphizing the mouse cardiac action potential via a novel dynamic clamp method. *Biophysical Journal* 2009;97(10):2684–2692.
- [8] Garry A, Hunter PJ. OpenCOR: a modular and interoperable approach to computational biology. *Frontiers in Physiology* 2015;6.
- [9] O’Hara T, Virág L, Varró A, Rudy Y. Simulation of the undiseased human cardiac ventricular action potential: Model formulation and experimental validation. *PLOS Computational Biology* 2011;7(5):e1002061.

Address for correspondence:

Alan Fabbri
 Department of Medical Physiology
 University Medical Center Utrecht
 Yalelaan 50, 3584CM Utrecht, The Netherlands
 afabbri@umcutrecht.nl